

Received: 2018.08.08  
Accepted: 2018.09.21  
Published: 2018.10.03

# Primary Cultivation and Identification of Vascular Smooth Muscle Cells from the Spiral Modiolar Artery of Guinea Pigs

Authors' Contribution:  
Study Design A  
Data Collection B  
Statistical Analysis C  
Data Interpretation D  
Manuscript Preparation E  
Literature Search F  
Funds Collection G

BCDF 1,2 **Jingjie Xiao\***  
BDE 1,3 **Zhiping Zhang\***  
BC 1,4 **Wei Zhang**  
CD 1,5 **Lei Wu**  
DE 1,2 **Liang Zhang**  
DF 1,2 **Yang Wang**  
DG 1,2 **Li Li**  
AEFG 1,6 **Xinzhi Li**  
AEFG 1,2 **Ketao Ma**

1 Key Laboratory of Xinjiang Endemic and Ethnic Diseases, Medicine School of Shihezi University, Shihezi, Xinjiang, P.R. China  
2 Department of Physiology, Medicine School of Shihezi University, Shihezi, Xinjiang, P.R. China  
3 Department of Otolaryngology, The First Affiliated Hospital, Medicine School of Shihezi University, Shihezi, Xinjiang, P.R. China  
4 Department of Gerontology, The First Affiliated Hospital, Medicine School of Shihezi University, Shihezi, Xinjiang, P.R. China  
5 Department of Cardiology, The First Affiliated Hospital, Medicine School of Shihezi University, Shihezi, Xinjiang, P.R. China  
6 Department of Pathophysiology, Medicine School of Shihezi University, Shihezi, Xinjiang, P.R. China

\* These authors contributed equally to this work

**Corresponding Author:** Ketao Ma, e-mail: maketao@hotmail.com, Xinzhi Li, email: lixinzhi@shzu.edu.cn

**Source of support:** This work was supported by the grants from the National Natural Science Foundation of China (31460264; 81460098; 81560175)

**Background:** This article reports a method to obtain vascular smooth muscle cells (SMCs) from the spiral modiolar artery (SMA) of guinea pigs and provides materials for related experimental studies.

**Material/Methods:** SMA was separated from the cochlea of guinea pigs, digested with trypsin (1.25 g/L) and allowed to adhere in a 35-mm culture dish. The morphology of the sample was investigated, and the sample was identified by immunofluorescence analysis, flow cytometry, Western blot, and RT-PCR. Cell viability was calculated using trypan blue and flow cytometry. Whole-cell patch clamp was used to record the membrane input resistance ( $R_{input}$ ), reciprocal membrane input conductance ( $G_{input}$ ), membrane input capacitance ( $C_{input}$ ), and resting membrane potential (RP) of the SMCs.

**Results:** Microscopy results showed that the cells had typical peak-valley growth pattern. The cell growth curve was similar to an S curve, and flow cytometry results showed that the cell apoptosis rate was less than 10%. Moreover, flow cytometry, immunofluorescent staining, Western blot and RT-PCR detected the specific and intensely positive expression of cell type-specific markers  $\alpha$ -SM-actin, SM22 $\alpha$ , calponin and desmin. Furthermore, following properties of the P3 and P6 cells were obtained:  $R_{input}$ , 2611 $\pm$ 356 and 2477 $\pm$ 338 M $\Omega$ ;  $G_{input}$ , 0.454 $\pm$ 0.071 and 0.273 $\pm$ 0.037 ns;  $C_{input}$ , 17.029 $\pm$ 0.917 and 18.042 $\pm$ 1.051 pF, and RP -20.602 $\pm$ 1.503 and -22.192 $\pm$ 1.905 mV.

**Conclusions:** Various highly purified SMCs were obtained from the SMA of guinea pigs. We provide an ideal experimental material for the study of the pathogenesis of diseases related to the circulation disturbances in the inner ear *in vitro*. The results can be used to evaluate the effects of drugs on vascular smooth muscle.

**MeSH Keywords:** Guinea Pigs • Myocytes, Smooth Muscle • Primary Cell Culture

**Full-text PDF:** <https://www.medscimonit.com/abstract/index/idArt/912606>



## Background

Numerous studies have shown that disorders in the circulatory system in the inner ear are closely linked to sudden deafness [1,2], Meniere's disease [3], senile hearing loss [4], and ototoxicity-induced hearing loss [5]. Moreover, the blood supply of the spiral modiolar artery (SMA) is believed to play a vital role in maintaining the function of the auditory apparatus because of the high energy consumption of auditory conduction process [6–8].

The SMA is the only artery responsible for supplying blood to the cochlea, the upstream arteries of which are the anterior inferior cerebellar artery and basilar artery. The former artery has 2 functional terminal branches, namely, the vestibular cochlear and spiral artery branches [9]. Hence, if abnormal changes occur in the SMA, such as vasospasm, this change would reduce or even completely interrupt the cochlear blood supply. This condition contributes to blood circulation disorders in the inner ear and cochlear dysfunction, such as dizziness, tinnitus, and other symptoms [8,10]. Hence, the blood supply of SMA may have a decisive impact on maintaining normal hearing [11]. The blood vessel wall is principally composed of an inner layer of endothelial cells (ECs), a medial layer of smooth muscle cells (SMCs), and an outer layer of fibroblasts. The blood flow is controlled effectively by the diameter of the blood vessel being regulated by the contractile activity of the SMCs [9]. However, the SMA cannot meet the requirements of related experiments, because it only has a single branch on each side, and the sample size is small [7]. Therefore, establishing a model of SMCs *in vitro* is highly significant to study the pathophysiological changes caused by disorders in the inner ear circulatory system and the etiological mechanism of relevant diseases.

Although SMCs has long been cultured, distinct differences have been observed in the structure and function of blood vessels among various organs or tissues. Moreover, we previously confirmed that the resting membrane potential (RP) of SMCs in the SMA exhibited a unique bimodal distribution [12,13]. Hence, conclusions drawn from the other organs or tissues cannot be fully applied to the inner ear circulatory system. We finally utilized a combination of enzymatic digestion and direct adherence protocols in this experiment to cultivate a large number of SMCs of the SMA. The results verified that the cells were in good condition with good cell viability. Thus, this provides an excellent model for the study of the physiology and pathology of the SMA *in vitro*.

## Material and Methods

### Animals

Guinea pigs (2 weeks old and 150–200 g) were purchased from the Animal Experimental Center of Xinjiang Medical University, China, and 3 guinea pigs were used per experiment. All animals with license lot number CXK New (2003-0001) were of the first-class standard. The feeding and experimental processes were performed with the approval of the Institutional Ethics Review Board of Shihezi University.

### Primary culture

Guinea pigs were anesthetised and then sacrificed by exsanguination. The iliac bones were removed under sterile condition, and the auditory blebs were separated and opened in physiological saline. The cochlea was removed under a microscope (Olympus Optical Co., Tokyo, Japan), and the capillary network and the spiral ligaments were removed from the outer wall of the cochlea. Thus, the SMA and its related radiating arterioles were further dissected from the cochlea with meticulous attention. Rapidly, the isolated SMA and its branches were placed in an ice-cold  $\text{Ca}^{2+}/\text{Mg}^{2+}$ -free Hanks' balanced salt solution (Solarbio Science and Technology Co., Beijing, China), rinsed 2–3 times, and transferred to a sterile bench. In order to ensure that the separated tissue pieces were sufficiently active, the operation of this part should be as fast as possible. Then, the blood vessel fragments were digested by trypsin (1.25 g/L) (Gibco, Carlsbad, CA, USA) in a  $\text{CO}_2$  incubator (Thermo Fisher Scientific, USA) for 20 min. To enhance enzymatic digestion, the Petri dish was gently shaken 3–4 times (5 min apart), and 5 mL of fetal bovine serum (FBS, 200 mL/L) (Gibco, Carlsbad, CA, USA) was added to stop trypsin digestion. The sample was centrifuged at 104.5 g for 5 min. The supernatant was discarded, and a few drops of the FBS medium was added to the remaining vessel fragments and spread evenly in the Petri dish. The gap of the blood vessel segment was approximately 2–3 mm. The culture dish was inverted and placed in the incubator for 2 h. Then, the dish was turned over, and DMEM/F-12 (Gibco, Carlsbad, CA, USA) was added. The dish was placed in the  $\text{CO}_2$  incubator for 3 days, during which the dish was not be moved. Fresh medium was replaced each day from day 4. On days 6–8, the cells grew from the edge of the tissue, and the culture vessel was overgrown by approximately 3 weeks.

### Cell inheritance

Cell passage was performed when the cell growth density reached 80% to 90% [14]. The cells were washed twice with PBS and digested with trypsin (2.5 g/L; containing 0.2 g/L EDTA). The cell edge refraction was enhanced, and the sheet became wrinkled and rounded. Then, the cell gap gradually became

bigger under microscopy. The digestion was terminated immediately when the cells were mostly detached, and the larger blood vessel fragments were discarded. The cell suspension was collected and centrifuged at 104.5 g for 5 min. The supernatant was discarded, and the medium was gently mixed by pipetting. The medium was transferred to 2 new 35-mm culture dishes, and the cells continued to grow in the incubator.

### Cell purification

The fibrous layers of the intima and outer layer could not be easily removed because of the small diameter of the SMA. Therefore, during cell passage, the cells were purified based on the different adherence times of the fibroblasts and SMCs. Another study has reported that fibroblasts had greater adherence than SMCs, and SMCs are larger than ECs [15,16]. Moreover, the ECS cannot survive under the above culture conditions, because they require higher culture conditions [17–19]. Hence, after 30 min of incubation at 37°C, the SMCs failed to attach to the culture dishes and could be collected with the supernatant. This process was repeated twice, and the liquid supernatant was collected for future cultures.

### Cell identification, morphological observation, and examination of cell viability

The size, shape, growth pattern, and myofilament of the cells were observed using a microscope. Afterwards, trypan blue (Sigma-Aldrich, St. Louis, MO, USA) was added to the cells, and the viable and dead cells were examined under an inverted light microscope.

### Flow cytometry

The cells in the logarithmic growth phase of the 3<sup>rd</sup> (P3) and 6<sup>th</sup> (P6) generations were uniformly planted into a 6-well plate. Then, the cell density was adjusted to  $1 \times 10^6$  cells/mL. On the one hand, the cells were collected, washed twice with PBS and resuspended with 500  $\mu$ L 1 $\times$ Bingding Buffer working solution. Then, Annexin V-FITC and PI were added using the Annexin V-FITC kit by following the manufacturer's instructions (MultiSciences Lianke Biotech Co., Ltd. China). The cells were shaken gently and mixed at 4°C for 30 min in the dark. Quantitative analysis of apoptosis proportion was conducted by flow cytometry (BD FACSAria™ III Cell Sorter No.648282, Becton Dickinson, USA). On the other hand, the cells were collected, washed twice with PBS, centrifuged at 104.5 $\times$ g for 5 min and resuspended with PBS. A blank tube and an isotype control tube were set at the same time. The appropriate antibodies (anti- $\alpha$ -SM-actin (Cat. No. ab124964; Abcam, UK), anti-SM22 $\alpha$  (Cat. No. ab10135; Abcam, UK), anti-calponin (Cat. No. ab700; Abcam, UK) and anti-desmin (Cat. No. ab15200; Abcam, UK)) were added according to the instructions. The cells were shaken gently and mixed at room temperature for 30 min in the

dark and centrifuged at 338 g for 6 min. The secondary antibodies were added in a dark room. The cells were incubated at 4°C for 30 min, washed twice with PBS, resuspended with PBS, and examined by flow cytometry.

### Immunofluorescence

The P3 and P6 cells in the logarithmic growth phase were uniformly plated in a 6-well plate, in which the slides were placed, and the cells were patched. After 3 days, the medium was discarded, and the cells were washed 3 times with PBS pre-warmed to 37°C and fixed in paraformaldehyde (40 g/L) for 15 min. The cells were again washed 3 times (5 min each time) with PBS and permeabilised by Triton-x-100 (2 mL/L) for 3 min. The cells were again washed 3 times (5 min each time) with PBS and incubated with BSA (50 g/L) at room temperature for 30 min. Then, the cells were washed 3 times (5 min each time) with PBS. The anti- $\alpha$ -SM-actin (Cat. No. ab124964; Abcam, UK), anti-SM22 $\alpha$  (Cat. No. ab14106; Abcam, UK), anti-calponin (Cat. No. ab46794; Abcam, UK), and anti-desmin (Cat. No. ab8470; Abcam, UK) were added, and the wet box was kept at 4°C overnight. The next day, the cells were re-warmed for 30 min at 37°C and washed 3 times (5 min each time) with PBS. Goat anti-rabbit or goat anti-mouse secondary antibodies (Sigma-Aldrich, St. Louis, MO, USA) were added in the dark, and the cells were incubated at 37°C for 1 h. The cells were washed 3 times (5 min each time) with PBS, and nuclei were stained with 4,6-diamino-2-phenyl indole (DAPI) (Solarbio Science and Technology Co., Beijing, China). Then, confocal microscopy (Zeiss LSM 510 META, Carl Zeiss AG, Germany) was performed to analyse the results.

### Western blot

The P3 and P6 cells in the logarithmic growth phase were uniformly plated in a 6-well plate, cracked, and estimated by a BCA protein assay. Each sample with equal amounts of protein (15  $\mu$ g/lane) was separated by 10% SDS-PAGE electrophoresis. The resolved proteins were then transferred to a PVDF membrane (Millipore, Billerica, MA, USA). The membranes were blocked with non-fat milk (50 g/L) in TBST buffer (pH 8.0, 10 mmol/L Tris-HCl, 150 mmol/L NaCl, and 0.2% Tween-20) for 1 h at room temperature and then probed with various primary antibodies (anti- $\alpha$ -SM-actin (Cat. No. ab124964; Abcam, UK), anti-SM22 $\alpha$  (Cat. No. ab14106; Abcam, UK), anti-calponin (Cat. No. ab46794; Abcam, UK), and anti-desmin (Cat. No. ab8470; Abcam, UK)) overnight at 4 °C. After the primary antibody incubation, the blots were washed 3 times (5 min each time) with TBST and incubated with the secondary antibody [1: 10 000; horseradish peroxidase-conjugated goat anti-rabbit or goat anti-mouse secondary antibodies (Beijing Fir Jinqiao Biotechnology Co., Beijing, China)] at room temperature for 2 h. Next, the blots were washed 5 times (5 min each time) with TBST and

**Table 1.** Primers applied.

Gene	Sequence(5'-3')	Product length (bp)
F-GAPDH	ATGTGTCCTCGTGGATCTGA	132
R-GAPDH	AGACAACCTGGTCTCAGTGT	132
F- $\alpha$ -SM-actin	TGGACTCTGGAGATGGCGTGAC	249
R- $\alpha$ -SM-actin	TTCATGGACCAGCATTCTTCC	249
F-SM22 $\alpha$	AGGAGAGTTCTAGGACAGCCAAGG	395
R-SM22 $\alpha$	TCGGTCGGTCCAGAGCAAGAG	395
F-Calponin	TTAAGGATTGCTGTGCGTCTAGG	270
R-Calponin	CACCAAGGCTGAGGAGGAGAGG	270
F-Desmin	TCTGTTTACCTCCCTACTCCA	218
R-Desmin	AGTGTTCATAGAAGGAGCAA	218

visualised on X-ray film using an ECL reagent (Cat. No. RPN2109; GE Healthcare Life Sciences, Chalfont, UK). The optical density of each target protein band was assessed with Quantity One software (Bio-Rad, Hercules, CA, USA) and normalised to the density of corresponding GAPDH bands in the same sample.

### RT-PCR

The P3 cells were detached with a solution of trypsin-EDTA, collected in a polypropylene round bottom tube, and centrifuged at 15 048 g for 5 min. RNA was extracted with an RNeasy micro kit, and cDNA was synthesised with an RETROscript kit (Thermo Fisher scientific, USA) for RT-PCR according to the manufacturer's instructions. The following reaction conditions were used for the RT-PCR: 60°C for 42 min; 70°C for 5 min; then held at 4°C. The genes of interest included  $\alpha$ -SM-actin, SM22 $\alpha$ , calponin, and desmin. Forward and reverse primers (Table 1) and reagents in the RETROscript kit were prepared according to the manufacturer's instructions. PCR products were separated and analyzed by 1.5% agarose gel electrophoresis.

### Whole-cell patch clamp

Whole-cell patch clamp experiments were performed using an Axon 700B amplifier (Molecular Devices, LLC, Sunnyvale, CA, USA) at room temperature. The cored borosilicate glass blank (Sutter Instrument Co., Ltd. Novato, CA, USA) was selected and made into a microelectrode using a P-2000 electrode drawing instrument (Sutter Instrument Co., Novato, CA, USA). The microelectrode with resistance of 2–8 M $\Omega$  was selected, and the electrode liquid (K-Gluconate 130 mM, NaCl 10 mM, MgCl<sub>2</sub>·6H<sub>2</sub>O 1.2 mM, CaCl<sub>2</sub> 2 mM, EGTA 5mM, HEPES 10 mM, and D-glucose 7.5 mM) was filled. The pH value was adjusted to 7.35–7.45

with 1 M KOH, and the osmotic pressure of sucrose was adjusted to 300–330. The glass microelectrode was filled with the intracellular fluid to the micromanipulator and gave a positive pressure with a 5-mL syringe. The micromanipulator was operated such that the tip of the microelectrode was close to and in contact with the cell, and the electrode resistance could be slightly increased from the film test window as soon as the cell was contacted. The electrode contacted with the cells with negative pressure and the clamping potential was adjusted to -40 mV. After the G $\Omega$  seal was formed between the cells and the electrode, the membrane was absorbed with the aid of negative pressure or electricity at the same time. After the membrane was broken, cells with resistance above G $\Omega$  were used for the experiment. The cell membrane capacitance current was not compensated to monitor cell membrane parameters online, and the membrane input resistance ( $R_{input}$ ) and membrane input capacitance ( $C_{input}$ ) of the cells were calculated. The exponential equation was used to simulate the film capacitor charging and discharging processes.

### Statistical analysis

All values are presented as Mean  $\pm$  SE. Differences between groups were assessed by one-way ANOVA and *t* test, as appropriate. *P* values less than 0.05 ( $P < 0.05$ ) were considered as indicating a significant difference.

## Results

### Cell culture

After the SMA vessel fragments were attached to the culture dish for 6 days, over 85% of the tissue pieces survived, and many cells were released from the edge of the tissue block (Figure 1A). After 10 days, as the cells proliferated, the cells grew in parallel in the culture dish and subsequently spread around the bottom of the dish for approximately 18 days (Figure 1B). Despite being in multiple distinct sizes and shapes, such as fusiform, triangular, or ribbon, the cells retained various lengths of cytoplasm, such as rich cytoplasm, nucleus oval, central, and even binuclear or multinuclear. When the cell density was low, the cells were often arranged in a net-like array and showed a typical peak-valley growth pattern after approximately 22 days (Figure 1C).

### Examination of cell viability

We calculated the cell viability and the total number of cells by trypan blue. The results were used to describe the growth curve of the cells. Notably, the cells grew to the logarithmic growth phase after 2–4 days, plateaued after 4–6 days, and slightly apoptosized in approximately 1 week. The SMC growth curve was a typical S curve (Figure 2).

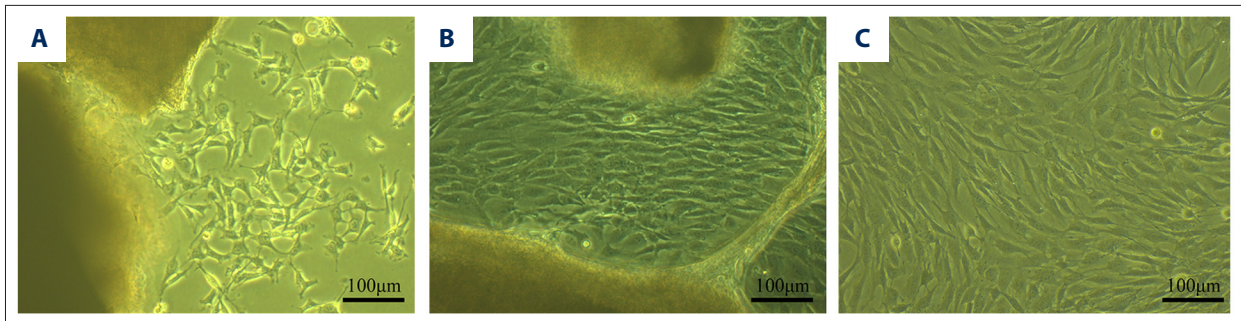


**Figure 1.** Growth process of SMCs (n=5). (A) On the 6<sup>th</sup> day of culture, the cells climbed out ( $\times 100$ ); (B) On the 18<sup>th</sup> day of culture, the cells covered the bottom of the dish ( $\times 100$ ); (C) The cells were typically in peak-valley growth pattern ( $\times 100$ ).

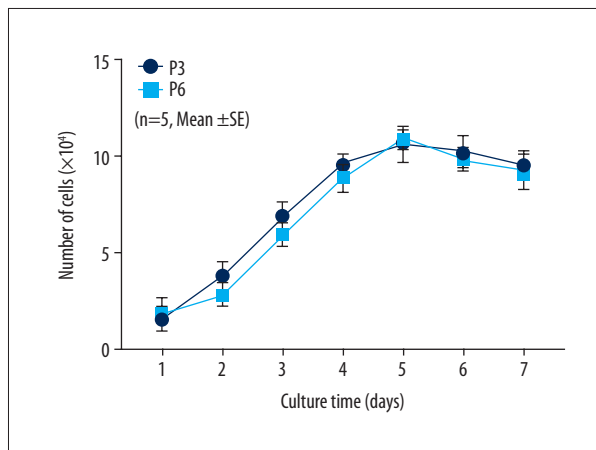


**Figure 2.** Growth curve of the SMCs. P3 (solid blue) and P6 (light blue) cell growth curves were similar to S curve.

### Flow cytometry

The P3 and P6 SMC cells were collected, and the apoptosis rates of each group were detected by flow cytometry. The results showed that the Q1 regions were characterised by necrotic cells mixed with a small number of late apoptotic cells or even those with mechanical damage. Likewise, the cells in the Q2 region represented late apoptotic cells, whilst the cells in the Q3

region represented the early apoptosis stage. Some cells in the Q4 region represented living cells. Among these regions, the cell apoptosis rate of the P3 of Q2+Q3 was  $6.9\% \pm 0.8\%$ , and the activity ratio of Q4 was  $92.3 \pm 1.8\%$  (Figure 3A). The cell apoptosis rate of the P6 of Q2+Q3 was  $7.4 \pm 0.8\%$ , and the activity rate was  $91.8\% \pm 1.2\%$  (Figure 3B). These apoptotic rates measured by flow cytometry were quantified and statistically analyzed (Figure 3C). In addition,  $98.8 \pm 1.1\%$  of the VSMCs were stained positively for  $\alpha$ -SM-actin, SM22 $\alpha$ , calponin, and desmin (Figure 4).

### Immunofluorescence

The P3 and P6 cells were cultured and stained with SMCs specific marker proteins ( $\alpha$ -SM-actin, SM22 $\alpha$ , calponin, and desmin).  $\alpha$ -SM-actin is a protein rich in SMCs, which is predominantly expressed in contractile cells. However, it is very low in synthetic cells. The SMCs are in a state of differentiation and maturity when the  $\alpha$ -SM-actin becomes the most abundant protein in these cells. SMCs of early differentiation are specific markers and are the most widely used contractile marker protein (Figure 5A, 5D). Then the nuclei had been counterstained with DAPI (Figure 5B, 5E), and merged (Figure 5C, 5F). SM22 $\alpha$  is a differentiation-related gene in the early stage of SMCs, and this gene is highly expressed in proliferating SMCs and lowly expressed in differentiated SMCs (Figure 6A, 6D).

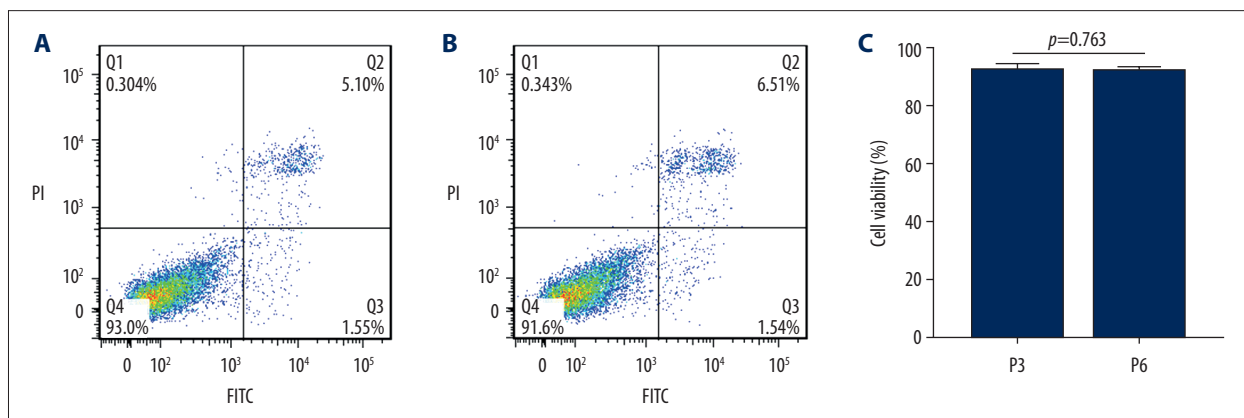


**Figure 3.** (A, B) Proportion of apoptosis and activity in the P3 and P6 SMCs; (C) Statistical analysis (n=3,  $p=0.763$ ).

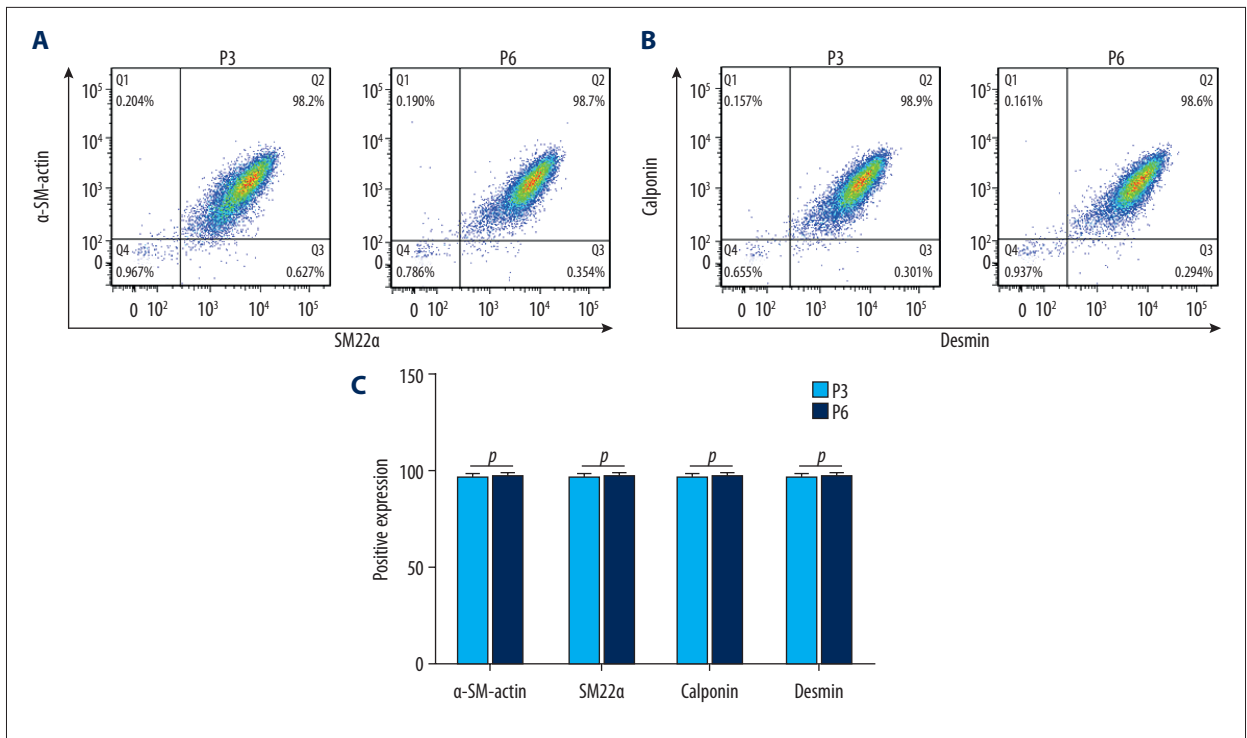


**Figure 4.** (A, B) Positive expression rate of  $\alpha$ -SM-actin, SM22 $\alpha$ , calponin and desmin in the P3 and P6 VSMCs; (C) Statistical analysis (n=3, all  $P>0.05$ ).

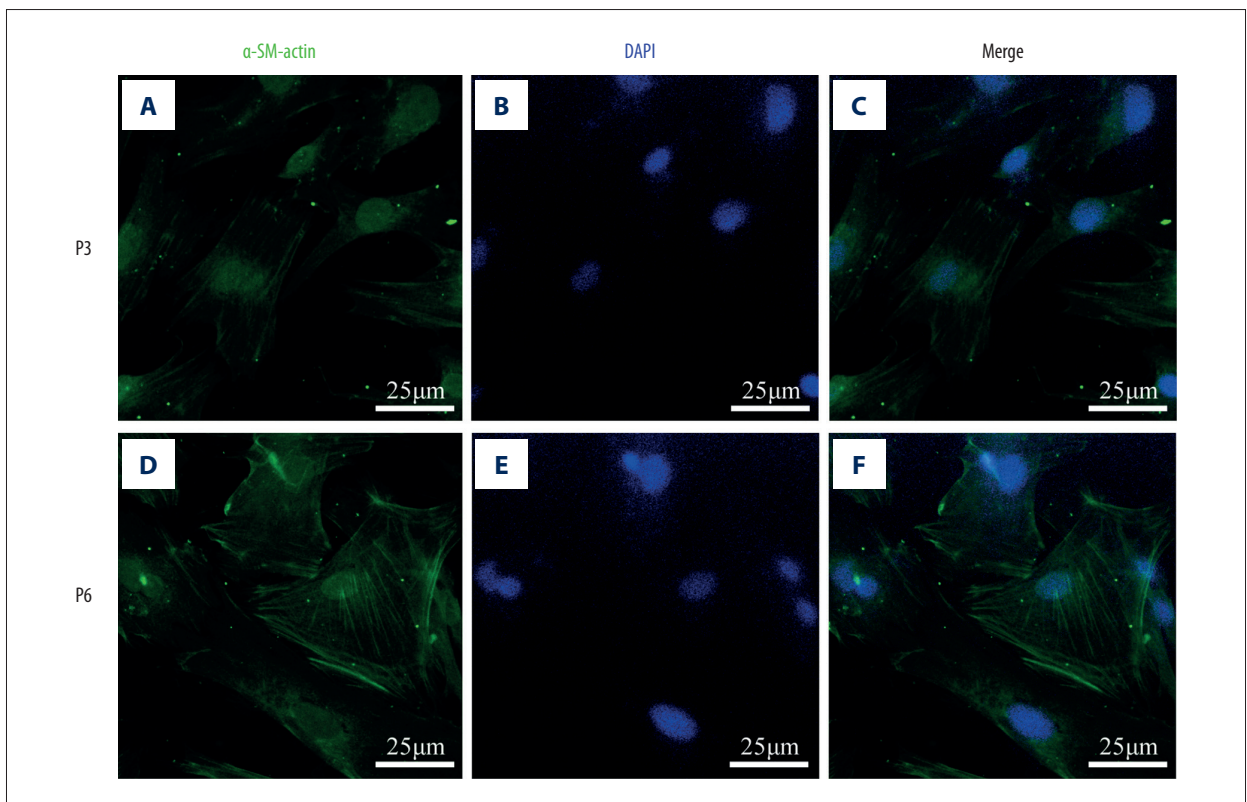


**Figure 5.** (A-F) Expression and location of  $\alpha$ -SM-actin (green) in the SMCs. Nuclei had been counterstained with DAPI (blue). Scale bar: 25  $\mu$ m.

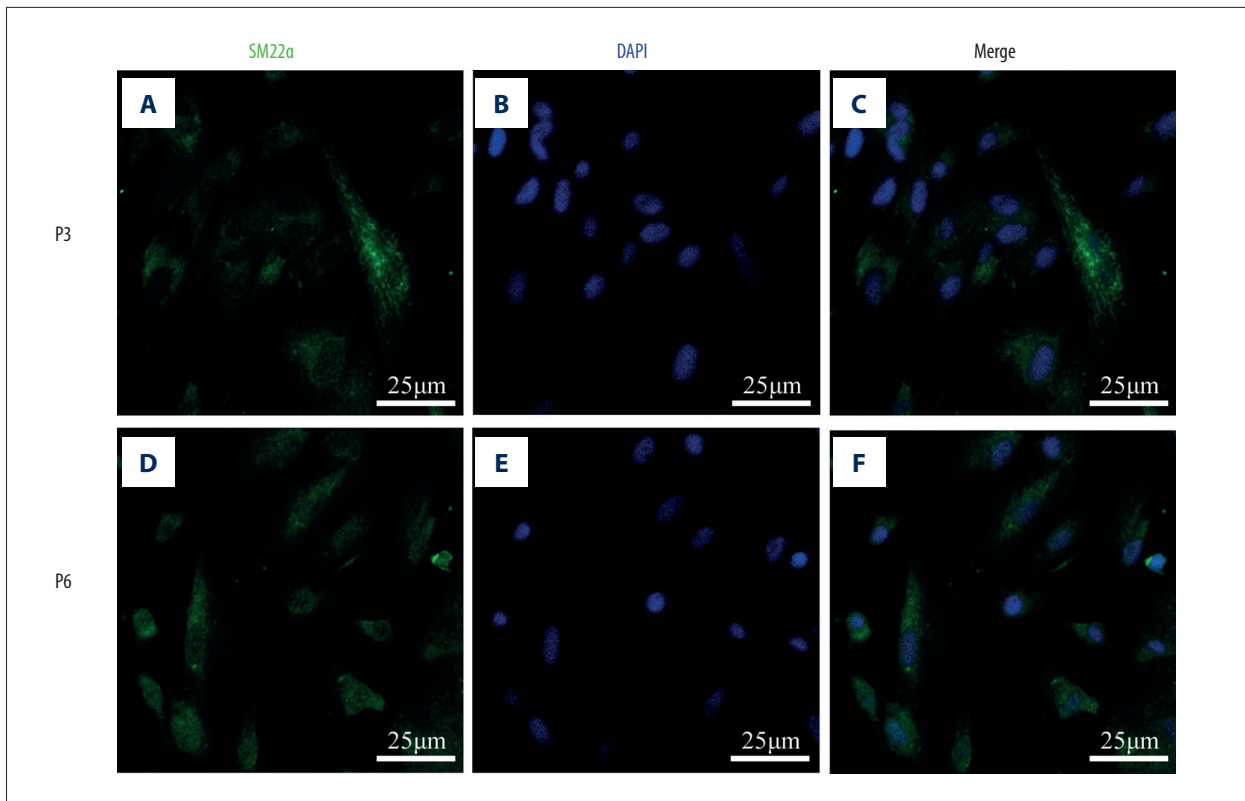


**Figure 6.** (A–F) Expression and location of SM22 $\alpha$  (green) in the SMCs. Nuclei had been counterstained with DAPI (blue). Scale bar: 25  $\mu$ m.

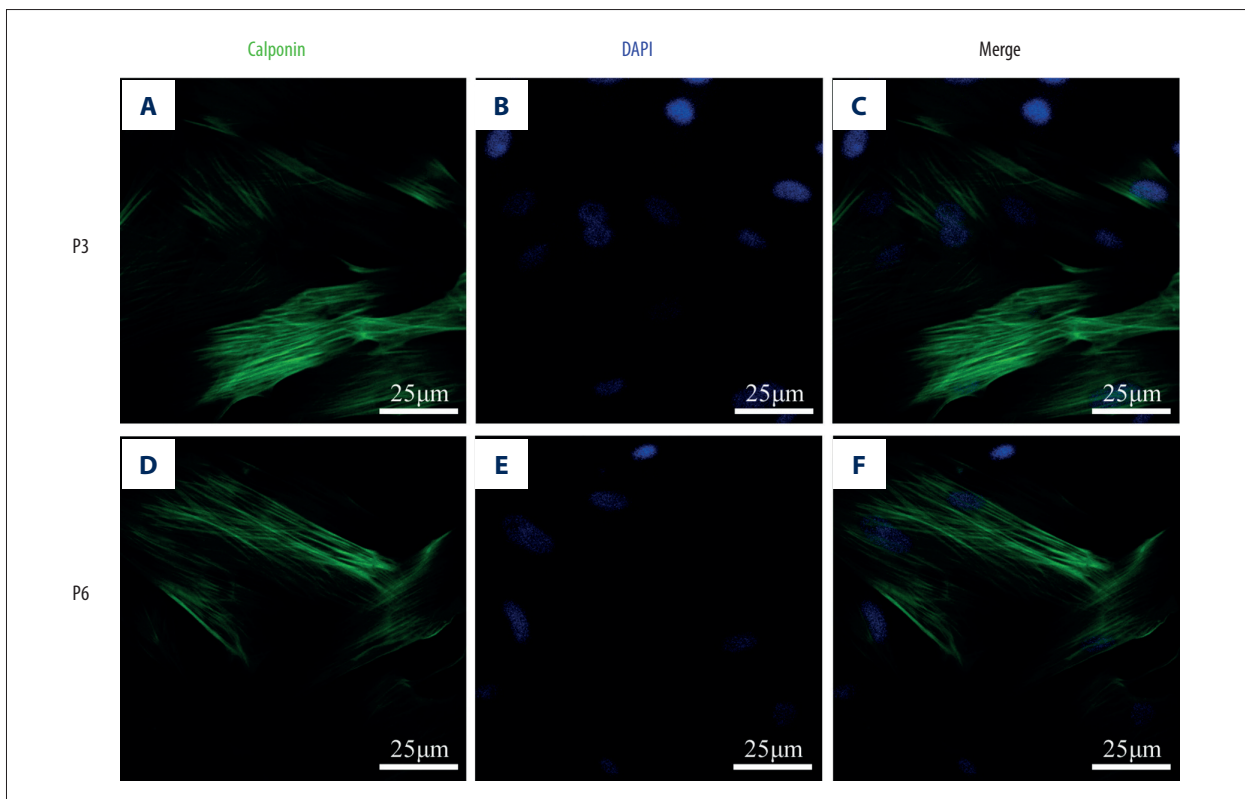


**Figure 7.** (A–F) Expression and location of calponin (green) in the SMCs. Nuclei had been counterstained with DAPI (blue). Scale bar: 25  $\mu$ m.

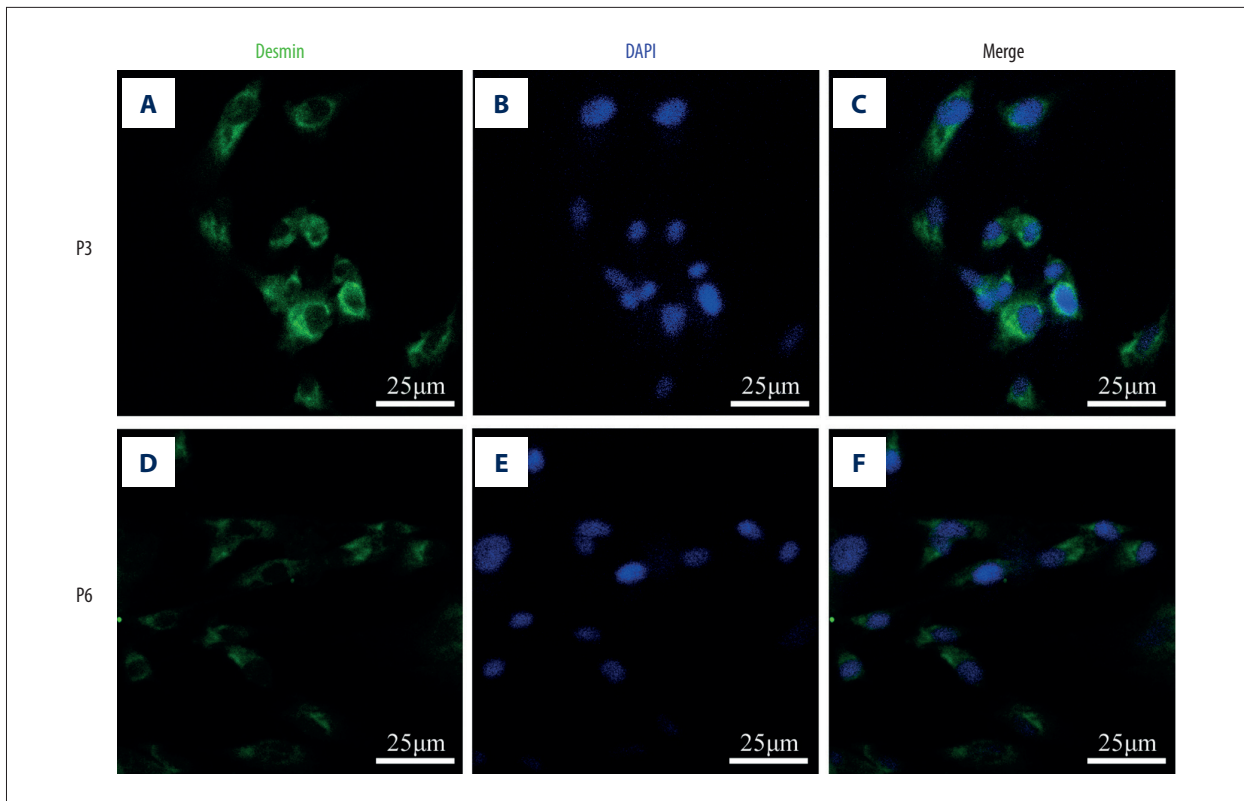


**Figure 8.** (A–F) Expression and location of desmin (green) in the SMCs. Nuclei had been counterstained with DAPI (blue). Scale bar: 25  $\mu$ m.

The nuclei had been counterstained with DAPI (Figure 6B, 6E), and merged (Figure 6C, 6F). Calponin is a characteristic protein of SMC, which is similar to tropomyosin in the smooth muscle tissue and is one-quarter of the  $\alpha$ -SM-actin (Figure 7A, 7D). And the nuclei had been counterstained with DAPI (Figure 7B, 7E), then merged (Figure 7C, 7F). Desmin is a polymer in which a dense body and a dense region inside the membrane form a complete intracellular framework (Figure 8A, 8D). Also, the nuclei had been counterstained with DAPI (Figure 8B, 8E), then merged (Figure 8C, 8F).

#### Western blot

The P3 and P6 cells were harvested, and the total protein was lysed and extracted. The expression of smooth muscle-specific markers ( $\alpha$ -SM-actin, SM22 $\alpha$ , calponin, and desmin) was detected by Western blot (Figure 9A). These protein bands were quantified and statistically analyzed (Figure 9B).

#### RT-PCR

The results revealed the corresponding RT-PCR gene analysis for SMCs. The marker genes of  $\alpha$ -SM-actin, SM22 $\alpha$ , calponin, and desmin were detected in the cells (Figure 10).

#### Whole-cell patch clamp

According to the whole-cell patch clamp experiments, we recorded the corresponding electrophysiological properties of the P3 and P6 SMCs (Figure 11A, 11B) as follows:  $R_{input}$ ,  $2611 \pm 356$  and  $2477 \pm 338$  M $\Omega$ ; reciprocal membrane input conductance ( $G_{input}$ ),  $0.454 \pm 0.071$  and  $0.273 \pm 0.037$  ns;  $C_{input}$ ,  $17.029 \pm 0.917$  and  $18.042 \pm 1.051$  pF; and RP,  $-20.602 \pm 1.503$  and  $-22.192 \pm 1.905$  mV (Table 2). We also recorded the scatter plot of the resting membrane potential of P3 and P6 from SMCs (Figure 12). These results were consistent with the experimental results of previous studies [20–22].

#### Discussion

To the best of our knowledge, the SMA is the only artery that supplies blood to the cochlea. This artery spirals up through the modiolus and is principally divided into 2 parallel capillary networks of the vascular stria and the spiral ligament in the lateral wall of the cochlea [9]. The densest capillary is found in the vascular stria. Given that the SMA is the only artery that supplies blood flow to the cochlea with less collateral circulation, once blockages occur, the blood flow is not easy to compensate and can result in disturbances and pathological damage of the microcirculation of the cochlea [23,24].

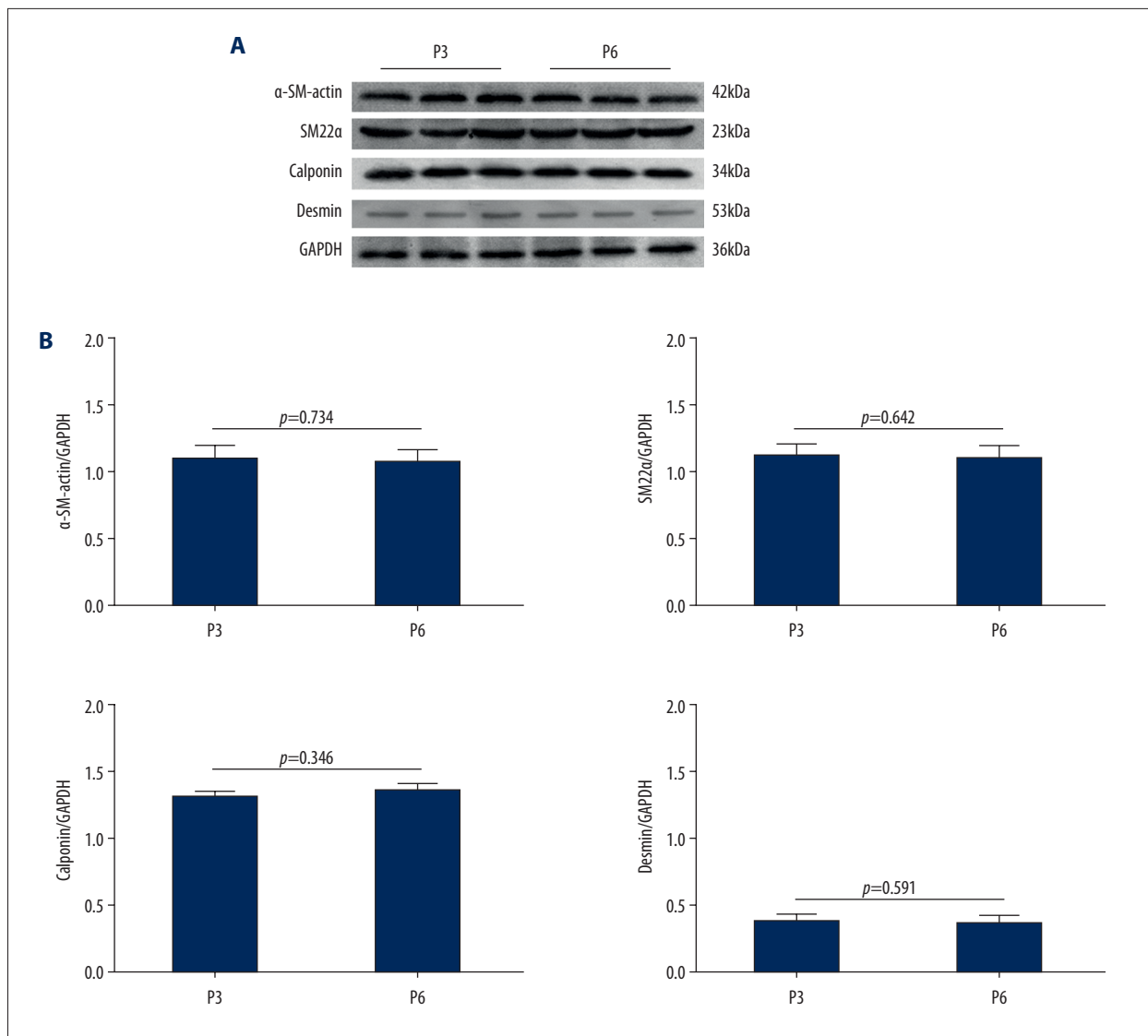


**Figure 9.** (A) Western blot analysis of  $\alpha$ -SM-actin, SM22 $\alpha$ , calponin, desmin and GAPDH protein expression in P3 and P6 SMCs; (B) Densitometry analysis (n=3, P=0.734, 0.642, 0.346, 0.591).

The supply of SMA blood flow plays a crucial role in maintenance of normal hearing [1–5]. Abundant evidence reveals that disorders in the circulatory system in the inner ear are closely correlated with sudden deafness, Meniere’s syndrome, senile hearing loss, ototoxic drug-induced hearing loss, and increased sensitivity to noise. Hence, the culture of SMCs is of great significance to study the underlying pathophysiological process of relevant diseases.

An approach for culturing SMCs has not been well established because of the small size and difficulty in separation of SMA. This limitation greatly restricts the study of the related pathophysiological changes in SMCs. The present experiment described in detail the separation of SMA and the method of culturing, purifying and identifying the primary cells. Hence,

a simple, economical, and efficient protocol for culturing SMCs of SMA has been established. In the laboratory investigation, we found that the SMCs were detached from the edge of the explants in approximately 6 days and reached confluence in approximately 18 days. Pure SMCs could be obtained from the third passage. After identification, the cell morphology showed the typical property of a peak–valley growth pattern. Immunofluorescence staining and flow cytometry demonstrated that the positive expression of specific markers in the P3 and P6 cells was over 95%. Moreover, the flow cytometry, Western blot, and RT-PCR results showed that special marker proteins and genes were also positively expressed. The results of trypan blue and flow cytometry showed that cells were in good condition and had good cell viability. In addition, the difference in the value of resting membrane potential between the

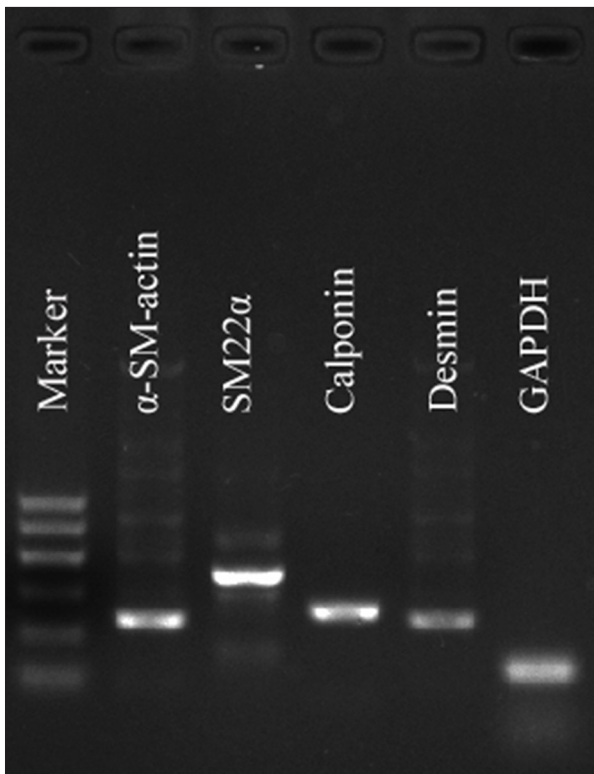


**Figure 10.** RT-PCR analysis of  $\alpha$ -SM-actin, SM22 $\alpha$ , calponin and desmin gene expression in the P3 SMCs.

acutely isolated SMCs in our earlier study and the cultured SMCs in the present study may be attributed to the type, concentration, and time of digestion of the enzyme selected for

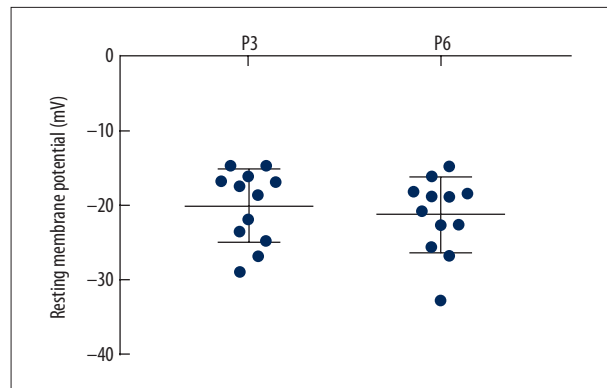


**Figure 12.** The scatter plot of the resting membrane potential of P3 and P6 from SMCs (n=12).

digesting the cells. We used a mixture of trypsin and collagenase IA (trypsin of 0.18 g/L and collagenase IA of 0.36 g/L) for the acutely isolated SMCs in our earlier study, and the digestion time was 5 min. By contrast, in the present study, we only used trypsin (2.5 g/L), and the digestion time was 90 to 120 s.

During culture, the purification of cells (i.e., the removal of the ECs and fibroblasts mixed in the SMCs to minimise contamination) was a major problem. Enzymatic digestion and explanting have been reported as the most common protocols for culturing SMCs [25–27]. Herein, cell cycle cultured by enzyme digestion method was short. However, the duration and concentration of used digestive enzyme remained difficult to determine. When the time for enzyme digestion was too short or enzyme concentration was too low, the digestion was not

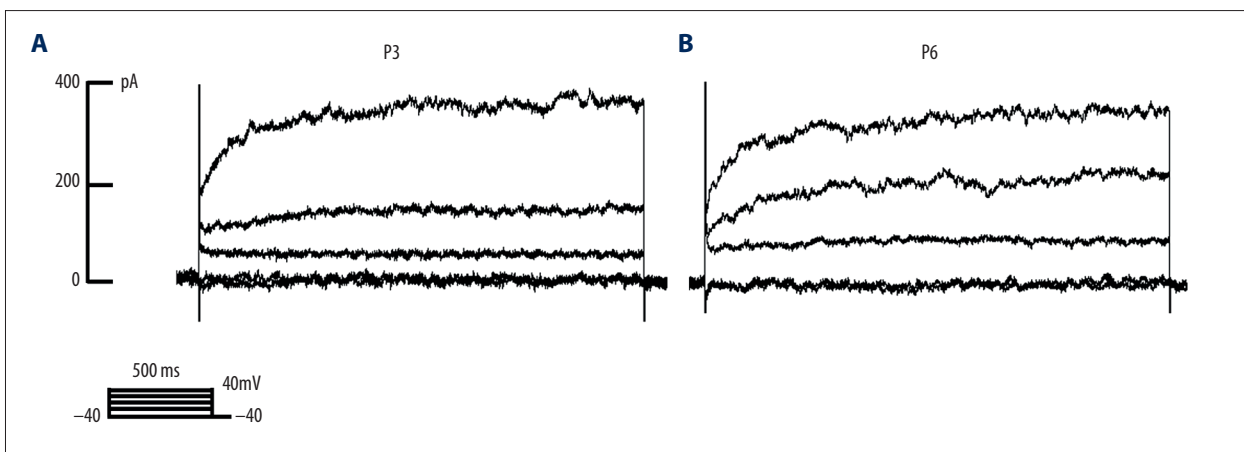


**Figure 11.** Electrophysiological properties of (A) P3 and (B) P6 from SMCs.

**Table 2.** Membrane electrophysiological properties of the SMCs of SMA.

Group	$R_{input}$ (M $\Omega$ )	$G_{input}$ (ns)	$C_{input}$ (pF)	RP (mV)
P3 (n=12)	2611 $\pm$ 356	0.454 $\pm$ 0.071	17.029 $\pm$ 0.917	-20.602 $\pm$ 1.503
P6 (n=12)	2477 $\pm$ 338	0.273 $\pm$ 0.037	18.042 $\pm$ 1.051	-22.192 $\pm$ 1.905

complete. By contrast, when the enzyme digestion time was too long or enzyme concentration was too high, cell damage was likely to occur. Furthermore, the enzyme itself has a toxic effect on the cells to some extent. Explanting is not only simple to perform but also less prone to contamination despite the longer culture cycle. The tiny arterial vessel wall is composed of 3 layers of cells, namely, the outer layer of fibroblasts, the medial layer of SMCs, and the inner layer of ECs. The large SMCs, fibroblasts, and ECs can be removed by mechanical scraping during culture. Nevertheless, the SMA is so thin that it is not suitable for explanting. Thus, in our study, we finally combined the 2 protocols after multiple attempts.

Several key steps in the experiment should be considered. Firstly, in the selection of animals, guinea pigs have a cochlear anatomy similar to humans. However, young guinea pigs possess a higher proliferative potential than older guinea pigs under the same conditions. Hence, for sufficient tissues to guarantee the results of the experiment, newborn guinea pigs approximately 2 weeks old were chosen in this study. Moreover, 2 parallel capillary networks of the vascular stria and the spiral ligament in the lateral wall are found in the cochlea in guinea pigs. SMA should be gently separated to avoid damage resulting from excessive vascular traction. Furthermore, the growth of cells was density-dependent. The experimental results showed that the adequate size of the explant was 1 mm<sup>2</sup>, and the appropriate distance was approximately 2–3 mm to ensure that the cells had enough growth space and maintain suitable growth density. Moreover, the time to upset the culture dish was 2 h during explanting. If the time was too short or long, the explant would not attach firmly or dry out, respectively. Most importantly, we consciously used a concentration of FBS (200 mL/L) for primary cell culture. A lower serum concentration would decrease the success rate of culture. In view of subculture, the serum concentration of initial passages could

be reduced to 150 mL/L, and the subsequent passages should be 100 mL/L. Further experiments with successive reduction in the concentrations of FBS are currently being conducted.

Disorders in the circulatory system in the inner ear have contributed to additional challenges for people, such as Meniere's syndrome, senile hearing loss, and ototoxic drugs-induced hearing loss. The culture method of SMCs as described in this article is relatively mature. Therefore, this study can provide an ideal experimental material for the study of the underlying pathophysiological changes *in vitro* induced by disorders in the inner ear circulatory system. The results can also be used to evaluate vascular smooth muscle drugs.

## Conclusions

In summary, various highly purified SMCs were obtained from the SMA of guinea pigs. We provide an ideal experimental material for the study of the pathogenesis of diseases related to the circulation disturbances in the inner ear *in vitro*. The results can be used to evaluate the effects of drugs on the vascular smooth muscle.

## Acknowledgements

The authors thank the Key Laboratory of Xinjiang Endemic and Ethnic Diseases, the Department of Physiology, and the Department of Pathophysiology of Shihezi University School of Medicine for their assistance.

## Conflicts of interest

None.

## References:

1. Yoshida T, Ikemiyagi Y, Ikemiyagi F et al: Anterior inferior cerebellar artery infarction misdiagnosed as inner ear disease. *B-ENT*, 2016; 12(2): 143–47
2. Hou ZQ, Wang QJ: A new disease: Pregnancy-induced sudden sensorineural hearing loss? *Acta Otolaryngol*, 2011; 131(7): 779–86
3. Attanasio G, Cagnoni L, Masci E et al: Chronic cerebrospinal venous insufficiency as a cause of inner ear diseases. *Acta Otolaryngol*, 2017; 137(5): 460–63
4. Kurtaran H, Acar B, Ocak E et al: The relationship between senile hearing loss and vestibular activity. *Braz J Otorhinolaryngol*, 2016; 82(6): 650–53
5. Niihori M, Platto T, Igarashi S et al: Zebrafish swimming behavior as a biomarker for ototoxicity-induced hair cell damage: A high-throughput drug development platform targeting hearing loss. *Transl Res*, 2015; 166(5): 440–50
6. Kariya S, Cureoglu S, Fukushima H et al: Comparing the cochlear spiral modiolar artery in type-1 and type-2 diabetes mellitus: A human temporal bone study. *Acta Med Okayama*, 2010; 64(6): 375–83
7. Samantha B, Keil R, Gayathri K et al: Calcium sparks in the intact gerbil spiral modiolar artery. *BMC Physiol*, 2011; 11(1): 15–22
8. Krishnamoorthy G, Reimann K, Wangemann P: Ryanodine-induced vasoconstriction of the gerbil spiral modiolar artery depends on the Ca<sup>2+</sup>-sensitivity but not on Ca<sup>2+</sup>-sparks or BK channels. *BMC Physiol*, 2016; 16(1): 6–17
9. Wangemann P, Kai W: Neurogenic regulation of cochlear blood flow occurs along the basilar artery, the anterior inferior cerebellar artery and at branch points of the spiral modiolar artery. *Hear Res*, 2005; 209(1–2): 91–96
10. Kaymakçi M, Acar M, Burukoglu D et al: The potential protective effects of 2-aminoethyl diphenylborinate against inner ear acoustic trauma: Experimental study using transmission and scanning electron microscopy. *J Int Adv Otol*, 2015; 11(1): 1–5
11. Onal M, Elsurur C, Selimoglu N et al: Ozone prevents cochlear damage from ischemia-reperfusion injury in guinea pigs. *Artif Organs*, 2017; 41(8): 744–52
12. Li L, Ke-Tao MA, Zhao L et al: [The characteristics of resting membrane potential on smooth muscle cells and endothelial cells in guinea pigs cochlea spiral artery.] *Zhongguo Ying Yong Sheng Li Xue Za Zhi*, 2012; 28(2): 128–32 [in Chinese]
13. Jiang ZG, Si JQ, Lasarev MR et al: Two resting potential levels regulated by the inward-rectifier potassium channel in the guinea-pig spiral modiolar artery. *J Physiol*, 2001; 537(3): 829–42

14. Zhou Y, Zhou JG, Qiu QY et al: [Effects of ClC-3 chloride channel on H<sub>2</sub>O<sub>2</sub>-induced apoptosis in rat aortic vascular smooth muscle cells.] Chinese Pharmacological Bulletin, 2006; 22(10): 1175–79 [in Chinese]
15. Biela SA, Su Y, Spatz JP et al: Different sensitivity of human endothelial cells, smooth muscle cells and fibroblasts to topography in the nano-micro range. Acta Biomater, 2009; 5(7): 2460–66
16. Li H, Chang J: Bioactive silicate materials stimulate angiogenesis in fibroblast and endothelial cell co-culture system through paracrine effect. Acta Biomater, 2013; 9(6): 6981–91
17. Song JW, Gu W, Futai N et al: Computer-controlled microcirculatory support system for endothelial cell culture and shearing. Anal Chem, 2005; 77(13): 3993–99
18. Ng CT, Yip WK, Mohtarrudin N et al: Comparison of invasion by human microvascular endothelial cell lines in response to vascular endothelial growth factor (VEGF) and basic fibroblast growth factor (bFGF) in a three-dimensional (3D) cell culture system. Malays J Pathol, 2015; 37(3): 219–25
19. Yuan Q, Li JJ, An CH et al: Biological characteristics of rat dorsal root ganglion cell and human vascular endothelial cell in mono- and co-culture. Mol Biol Rep, 2014; 41(10): 6949–56
20. Ma KT, Guan BC, Yang YQ et al: 2-Aminoethoxydiphenyl borate blocks electrical coupling and inhibits voltage-gated K<sup>+</sup> channels in guinea pig arteriole cells. Am J Physiol Heart Circ Physiol, 2011; 300(1): H335–46
21. Ma KT, Li XZ, Li L et al: Role of gap junctions in the contractile response to agonists in the mesenteric artery of spontaneously hypertensive rats. Hypertens Res, 2014; 37(2): 110–15
22. Li XZ, Ma KT, Guan BC et al: Fenamates block gap junction coupling and potentiate BKCa channels in guinea pig arteriolar cells. Eur J Pharmacol, 2013; 703(1–3): 74–82
23. Jiang Y, Chen Y, Yao J et al: Anatomic assessment of petrous internal carotid artery, facial nerve, and cochlea through the anterior transpetrosal approach. J Craniofac Surg, 2015; 26(7): 2180–83
24. Kurata N, Schachern PA, Paparella MM et al: Histopathologic evaluation of vascular findings in the cochlea in patients with presbycusis. JAMA Otolaryngol Head Neck Surg, 2016; 142(2): 173–78
25. Metz RP, Patterson JL, Wilson E: Vascular smooth muscle cells: Isolation, culture, and characterization. Methods Mol Med, 2001; 46: 237–45
26. Salabei JK, Cummins TD, Singh M et al: PDGF-mediated autophagy regulates vascular smooth muscle cell phenotype and resistance to oxidative stress. Biochem J, 2013; 451(3): 375–88
27. Van NE, Pollet A, Den JT et al: A biomimetic microfluidic model to study signalling between endothelial and vascular smooth muscle cells under hemodynamic conditions. Lab Chip, 2018; 18(11): 1607–20